*Journal homepage: www.fia.usv.ro/fiajournal*
*Journal of Faculty of Food Engineering,*
*Ştefan cel Mare University of Suceava, Romania*
*Volume XXV, Issue 1- 2026,* pag. 66 - 76

FOOD AND ENVIRONMENT SAFETY

# OPTIMIZING FUNCTIONAL AND QUALITY ATTRIBUTES OF SLOE BERRY POMACE POWDER: A STUDY ON THE THERMAL TREATMENT AND GRANULOMETRY

**Mădălina UNGUREANU-IUGA [1,2], Mariana SPINEI[1*], Mircea Adrian OROIAN[3]**
[1]*Institute of Advanced Studies, Integrated Research, Development and Innovation Center for Advanced Materials, Nanotechnologies and Distributed Manufacturing and Control Systems (MANSiD), "Ştefan cel Mare" University of Suceava, 13 Universităţii Street, 720229 Suceava, Romania;*
[2] *Mountain Economy Center (CE-MONT), National Institute of Economic Research (INCE), Romanian Academy, 49 Petreni Street, 725700, Vatra Dornei, Romania*
[3]*Faculty of Food Engineering, "Ştefan cel Mare" University of Suceava, 13 Universităţii Street, 720229 Suceava, Romania;*
*Corresponding author: mariana.spinei@fia.usv.ro
Received 16 November 2025, accepted 31 March 2026

**Abstract:** *Physical and functional properties of sloe berry pomace (SBP) – a recoverable by-product – depend on the physical treatments applied. This paper aimed to highlight the impact of thermal treatment temperature (45, 55, 65 °C) used to reduce SBP moisture, along with particle size (L < 200 µm, 200 µm < M < 300 µm, L > 300 µm), on its color, functional properties, fiber content and protein secondary structure assessed by FT-IR. Response Surface Methodology was used for the experimental design, and the desirability function was employed to establish the optimal processing conditions. The results revealed that the increase in temperature determined an increase in L*, fiber content, water absorption and retention, and β-sheet conformation of protein for all the fractions studied. Both factors (temperature and particle size) exhibited significant impact (p < 0.05) on SBP color, functional properties, fiber content, and protein secondary structure, except for solubility index and β-turn conformations, which were not affected by temperature. The optimal thermal treatment conditions for each particle size were: 64.82 °C for L, 49.48 °C for M, and 45.19 °C for S. Optimal S fraction presented the best color, functional properties, and the most stable protein conformations. The optimal processing parameters identified provide a practical foundation for upcycling SBP into a valuable, functional food ingredient with tailored properties, such as enhanced fiber content and water-holding capacity, for use in the food and nutraceutical industries.*

**Keywords**: *sloe berry, by-product valorization, response Surface Methodology, functional properties, protein structure.*

## 1. Introduction

The sloe berry fruit (*Prunus spinosa* L.), also known as blackthorn, is a wild-growing member of the *Prunus* genus (Rosaceae family) appreciated for its potential as a source of natural bioactive compounds. The by-product resulting from sloe berry processing retains a great amount of these compounds. The effective utilization of this by-product, particularly by transforming it into shelf-stable powders, requires careful control over processing parameters like drying and subsequent particle size reduction. The nutritional composition of sloe berries includes sugars, organic acids, proteins, and cellulose [1]. Sloe berry is a source of essential minerals (K, P, Fe, Cu, and Na). Specific analysis showed high levels of K, P, and Mg. The fruits also contain provitamin A and Vitamins B1, B2, PP, and C [1]. Sloe berry fruits are characterized by containing fatty acids, predominantly polyunsaturated fatty acids over monounsaturated fatty acids [2]. The fruit is rich in highly valuable bioactive compounds, including polyphenols, tannins, and anthocyanins [3]. Drying is

*DOI: https://doi.org/10.4316/fens.2026.07*

critical for reducing excess water to safe limits and increasing the shelf life of perishable sloe berry fruits. Hot air thermal treatment is widely used due to its low capital and operational costs. However, this method involves thermal processes that can significantly impact the quality and composition of the final powder [4]. Thermal treatment, which causes dehydration at high temperatures, can induce the formation of non-polyphenolic compounds, specifically Maillard Reaction Products [5]. Thermal treatment by hot-air can lead to a higher L* value (lightness), which may be a result of pigment degradation in the presence of oxygen during the drying process, causing the color to lighten [4]. The thermal processing involved in drying leads to the degradation of valuable components. Hot-air thermal treatment negatively affects the retention of phenolic compounds and antioxidant activity [5]. Despite the loss of some bioactives, hot-air thermal treatment powder may offer a significant advantage due to its inherent stability, low production cost, and the ease of manufacture using simple equipment [4]. The fractionation process influences stability and functionality. Water Absorption Capacity values are clearly influenced by particle size; the decreasing particle size resulted in higher absorption capacity. This improvement is attributed to the breakdown of cell walls during grinding, which exposes hydrophilic groups and increases surface area [3]. Smaller particle sizes generally resulted in improvement in the solubility index. Powders with smaller particles should be more soluble and interact with water readily, which could aid in incorporation into food [6]. The careful control of the drying intensity and the post-drying selection of particle sizes allows producers to target specific functional characteristics, whether maximizing extraction efficiency or preserving labile nutrients, for optimized product development [3].

This paper aimed to evaluate the impact of thermal treatment conditions (temperature), applied to reduce SBP moisture, along with particle size, on the physical and functional properties of sloe berry pomace. For this purpose, color, functional properties, fiber content, and secondary structure of proteins by FT-IR were evaluated. Response Surface Methodology was used to evaluate the effects of factors, and an optimization was performed based on a desirability function.

## 2. Materials and methods

### 2.1. Materials

The process of transforming freshly collected sloe berries into precisely sloe berry pomace (SBP) powders involved sequential steps designed for juice extraction and subsequent analysis preparation. After the 2024 harvest in the Botoşani region of Romania, the berries were initially scalded and left for 24 hours before mechanical pressing.

Thermal treatment was applied to reduce moisture (< 6%) at different temperatures (45, 55, and 65 °C). Finally, the dried SBP was ground and systematically sieved into three distinct particle size fractions: small (S < 200 μm), medium (200 μm < M < 300 μm), and large (L > 300 μm), which were stored at 4 °C until they could be analyzed.

### 2.2. Analysis of color parameters

The color of the SBP powders was measured using a Konica Minolta CR-400 colorimeter in reflectance mode to quantify lightness *L** (0=black, 100=white), the red-green axis (a*), and the yellow-blue axis (b*). Browning index was calculated according to the method described by Al-Hilphy et al. [7].

### 2.3. Analysis of fiber content

The total crude fiber content was assessed by using an automated analyzer (Fibertec 2010, Tecator, Hillerod, Sweden).

**2.4. Analysis of functional properties**

The analysis of SBP powders included three main procedures to characterize their interaction with water: Water Absorption Capacity (WAC), Solubility Index (SI), and Water-Retention Capacity (WRC). The WAC test, involved mixing a 2.5 g sample with 30 mL of distilled water, followed by agitation in a 30 °C water bath for 30 minutes. The suspension was then centrifuged at 3500 rpm for 15 minutes, after which the supernatant was discarded, and the weight of the water-saturated residue was recorded to calculate the WAC percentage, adapting a method from [8].

The Solubility Index (SI), was determined using the supernatant collected from the WAC test. This liquid was dried in glass containers at 100 °C until it reached a constant mass. After cooling, the weight of this dried residue was measured [8].

The Water-Retention Capacity (WRC) was assessed using the method by Zhu et al. [9]. A 1 g sample was thoroughly mixed with 30 mL of distilled water and allowed to hydrate for an extended period of 18 hours. The mixture was then subjected to centrifugation at 3000 rpm for 20 minutes. The WRC was calculated based on a two-step weighing process: first, the remaining wet residue was weighed after removing the supernatant; second, this residue was dried at 105 °C for 2 hours and weighed again.

**2.5. Analysis of secondary structure of protein by FT-IR**

The structural characterization of SBP powders and their extracted oil was carried out using Fourier-transform infrared (FT-IR) spectroscopy (Thermo Scientific Nicolet iS20). Spectra were acquired from 650 to 4000 $cm^{-1}$ at a resolution of 4 $cm^{-1}$ over 32 scans to evaluate the effects of various treatment conditions and particle size fractionation.

Specifically, for SBP powders, the Omnic software was used to apply automatic Fourier deconvolution to the Amide I region (1585–1835 $cm^{-1}$) to analyze the protein secondary structure, calculating the proportion of spectral bands corresponding to structures such as intermolecular associations (1613–1620 $cm^{-1}$), $\beta$-sheets (1620–1644 $cm^{-1}$), and $\alpha$-helices (1650–1660 $cm^{-1}$) relative to the total Amide I area [10–12].

**2.6. Statistics and experimental design**

In this study, a factorial design of experiments (DoE) was employed to evaluate the effect of temperature and particle size on the selected response variable. For this, Response Surface Methodology with I-optimal design type and quadratic mathematical model was used. Temperature was considered as a numeric factor, varied between 45 °C and 65 °C, with a center point at 55 °C, while particle size was treated as a categorical factor with three levels (S, M, and L). The numeric factor levels were coded to standard values of −1, 0, and +1 to facilitate statistical analysis and response modeling. Experiments were conducted at all combinations of factor levels, and the corresponding response values were recorded. This design allowed for the assessment of both main effects and interactions, enabling the identification of optimal conditions for the desired characteristic of SBP. The optimization of temperature for each particle size was done using desirability function. The comparisons between the optimal samples were made using ANOVA with Tukey test, at a significance level of 95%.

Mathematical modeling and optimization were done using Design Expert software (trial version, Stat-Ease, Inc, Minneapolis, MN, USA), while other data processing was made in XL STAT (2024 version, Lumivero, LLC, Denver, CO, USA).

**3. Results and discussion**

**3.1. Effects of thermal treatment and granulometry on SBP properties**

Thermal treatment and particle size exhibited significant influences ($p < 0.05$)

on SBP properties. The quadratic models proposed for color, fiber content, functional properties and protein structure variations were suitable for prediction, with $R^2$ between 0.88 and 0.99 (Table 1). SBP lightness (L*) was significantly affected by both thermal treatment temperature and particle size ($p < 0.05$), while their interaction exhibited a non-significant effect. The increase in temperature up to 60 °C led to an increase in L* (eq. 1-3), then it decreased for all particle sizes (Fig. 1a). S particle presented the highest L* values, followed by L and M. It can be observed from Fig. 1b that Browning index (BI) decreased with temperature for S and L fractions, while for M it increased significantly ($p < 0.05$). S particle size presented the highest BI. Both factors and their interactions showed significant impact on BI (Table 1).

The increase in lightness (L*) of sloe berry pomace (SBP) up to 60 °C can be attributed to moisture loss and enhanced light scattering from finer particles, which increase reflectance and apparent brightness [13]. Above this temperature, non-enzymatic browning reactions, mainly Maillard reaction, caramelization, and phenolic oxidation, produce dark pigments that reduce L* values [5]. Smaller particles exhibited the highest L* and BI due to their greater surface area, promoting both light scattering and pigment formation upon heating. Similar results have been reported for apple, blueberry, and plum pomaces, where fine fractions showed higher L* but more intense browning after extended heating [14]. The prediction models for BI depending on the temperature for each particle size are displayed below (eq. 4-6).

L particle:

$$L^* = 21.63 + 1.13A - 0.01A^2 \quad (1)$$

M particle:

$$L^* = 19.31 + 1.12A - 0.01A^2 \quad (2)$$

S particle:

$$L^* = 20.07 + 1.13A - 0.01A^2 \quad (3)$$

L particle:

$$BI = 73.89 - 1.00A + 0.01A^2 \quad (4)$$

M particle:

$$BI = 55.93 - 0.73A + 0.01A^2 \quad (5)$$

S particle:

$$BI = 77.93 - 1.09A + 0.01A^2 \quad (6)$$

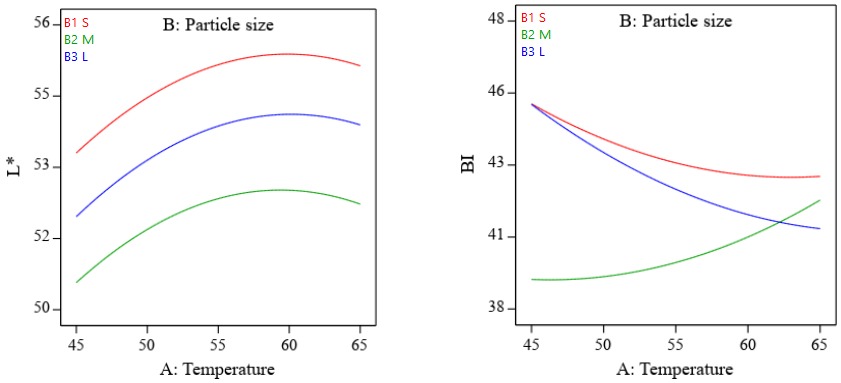


**Fig. 1. Interaction plot of thermal treatment temperature and particle size effects on SBP color parameters**

Both temperature and particle size, as well as their interaction, significantly affected ($p < 0.05$) SBP fiber content (Table 1).
The increase in temperature from 50 to 65 °C led to an increase in fiber content in all particle sizes (Fig. 2). The highest fiber content was observed in L particle size. The fact that the largest particle size (L) showed the highest fiber particle size (L) showed the highest fiber particle size (L) showed the highest fiber content is consistent with findings in pomace systems

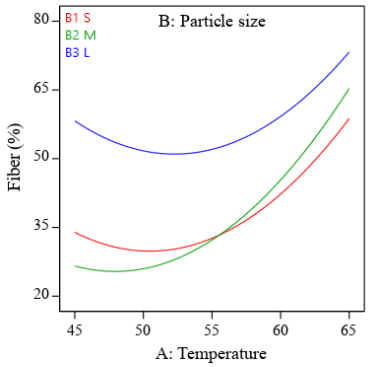


**Fig. 2. Interaction plot of thermal treatment temperature and particle size effects on SBP fiber content**

where coarser fractions retain more insoluble fiber (as finer particles tend to release or convert more of the insoluble fiber into other fractions or degrade) [15]. Moreover, moderate heating can increase total dietary fiber and insoluble fiber content, by inducing aggregation and cross-linking of polysaccharide components making them less extractable in the non-fiber fraction and thus quantified as fiber [16]. The following equations (eq. 7-8) descried the prediction model for fiber content in function of temperature for each particle size.

L particle:

$$Fiber\ (\%) = 379.28 - 13.85A + 0.14A^2 \quad (7)$$

M particle:

$$Fiber\ (\%) = 340.60 - 13.15A + 0.14A^2 \quad (8)$$

S particle:

$$Fiber\ (\%) = 425.63 - 14.34A + 0.14A^2 \quad (9)$$

Water absorption capacity (WAC) was influenced significantly ($p < 0.05$) by both factors and their interaction (Table 1). For S and L particle sizes, WAC increased with temperature increase, while for M samples, the opposite trend was recorded (Fig. 3a). The highest WAC was obtained for the S particle size, followed by M and L. The increase in temperature leading to higher water absorption capacity (WAC) can be explained by enhanced structural opening and dehydration of matrix components: as heating loosens cell walls and removes bound moisture, more hydrophilic sites become available for water binding, particularly in finer particles, which offer greater surface area. The fact that S had the highest WAC, followed by M and then L, is consistent with studies showing finer particle sizes generally increase WAC due to higher surface area and disrupted structure, and that water absorption is strongly influenced by particle size and porosity [17,18]. Furthermore, pomace and fiber-rich powders show elevated WAC as fiber content increases and hydrophilic groups become more accessible [19]. The prediction models are displayed in eq. 10-12.

L particle:

$$WAC\ (\%) = -14.86 + 9.01A - 0.06A^2 (10)$$

M particle:

$$WAC\ (\%) = 128.19 + 6.00A - 0.06A^2 (11)$$

S particle:

$$WAC\ (\%) = 13.55 + 7.19A - 0.06A^2 \quad (12)$$

Solubility index (SI) was significantly affected ($p < 0.05$) only by particle size and the interaction between factors. L fraction exhibited considerably lower SI compared to M and L (Fig. 3b). The lower solubility index (SI) observed in the large (L) particle fraction compared to medium (M) and small (S) fractions can be attributed to the higher proportion of intact cell wall and fibrous material in coarser particles, which resist hydration and dissolution. Smaller and medium particles, having more disrupted structures and higher surface area, allow greater water penetration and swelling, thereby increasing solubility [20]. Similar trends have been reported for fruit pomaces and plant by-products, where finer fractions exhibit higher solubility due to exposure of polysaccharides and proteins that can dissolve or disperse in water, while coarser fractions retain more insoluble fiber, limiting their solubility [21]. The prediction models for SI depending on

temperature for each particle size are shown in eq. 13-15.

L particle:

$$SI\ (\%) = -31.18 + 1.591A - 0.02A^2 \quad (13)$$

M particle:

$$SI\ (\%) = -35.83 + 1.661A - 0.02A^2 \quad (14)$$

S particle:

$$SI\ (\%) = -35.72 + 1.551A - 0.02A^2 \quad (15)$$

**Table 1.**

**Results of the REML (REstricted Maximum Likelihood) analysis**

| Factor | *F*-value | | | | | | | | |
|---|---|---|---|---|---|---|---|---|---|
| | L* | BI | Fiber | WAC | SI | WRC | *β*-sheet | *α*-helix | *β*-turn |
| *Whole-plot* | 32.99** | 7.79** | 340.63** | 18.99** | 75.86** | 16.75** | 5.89* | 3.60* | 5.62* |
| A-Temperature | 48.45** | 10.74** | 498.88** | 34.69** | 1.23 | 11.68** | 7.22* | 6.16* | 3.83 |
| $A^2$ | 17.53** | 4.84* | 182.38** | 3.47 | 150.49** | 21.81** | 4.59 | 1.04 | 7.40* |
| *Subplot* | 29.62** | 31.80** | 110.35** | 197.78** | 717.10** | 146.60** | 144.99** | 236.38** | 185.52** |
| B-Particle size | 59.14** | 37.41** | 186.26** | 358.90** | 1410.77** | 276.43** | 224.65** | 471.52** | 362.09** |
| AB | 0.10 | 26.19** | 34.44** | 36.61** | 23.42** | 16.77** | 64.56** | 1.24 | 8.95** |
| *Model evaluation* | | | | | | | | | |
| $R^2$ | 0.90 | 0.88 | 0.98 | 0.98 | 0.99 | 0.97 | 0.97 | 0.98 | 0.97 |
| Adj.-$R^2$ | 0.86 | 0.82 | 0.97 | 0.97 | 0.99 | 0.96 | 0.96 | 0.97 | 0.97 |

* – model term is significant at $p < 0.05$, ** – model term is significant at $p < 0.01$, BI – browning index, WAC – water absorption capacity, SI – solubility index, WRC – water retention capacity.

Water retention capacity (WRC) of SBP was significantly influenced by both factors and their interaction (Table 1). WRC increased with temperature rise up to 55 °C, then it decreased (Fig. 3c).

S and M particle sizes presented considerably higher WRC values compared to the L fraction. Water retention capacity (WRC) increased with heating up to 55 °C, likely due to partial swelling of fiber and exposure of hydrophilic groups, which enhance water binding [16]. Above 55 °C, WRC decreased, probably because further heating caused structural collapse or aggregation of fibrous components, reducing the number of accessible binding sites [22].

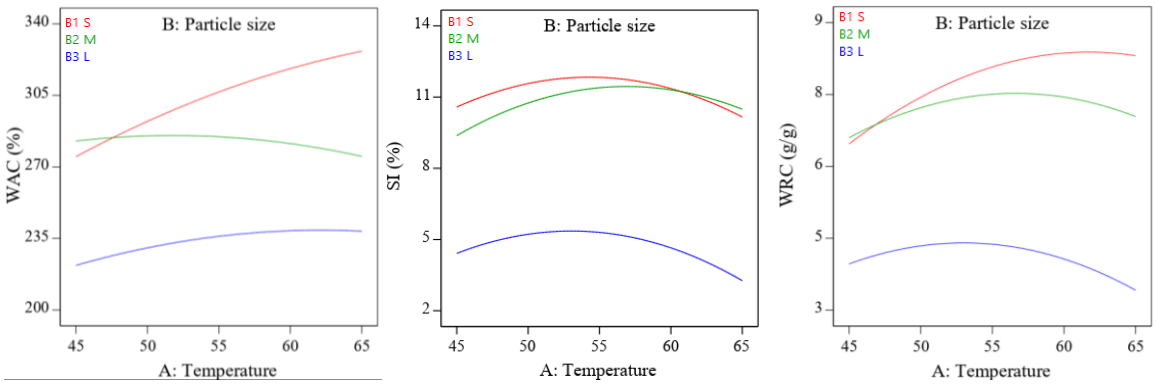


**Fig. 3. Interaction plot of thermal treatment temperature and particle size effects on SBP functional properties**

Small (S) and medium (M) particle fractions exhibited higher WRC than the large (L) fraction, which is consistent with studies showing that finer particles and moderately sized fractions have more exposed surface area and disrupted structures, promoting water retention, while coarser particles retain more intact cell walls that limit water uptake [20,21]. Eq. 16-18 show the prediction models for WRC depending on temperature for each particle size.

L particle:
$WRC\,(g/g) = -17.72 + 0.85A - 0.01A^2$ (16)
M particle:
$WRC\,(g/g) = -14.43 + 0.78A - 0.01A^2$ (17)
S particle:
$WRC\,(g/g) = -14.84 + 0.73A - 0.01A^2$ (18)

Heating of SBP powders can determine changes of the secondary structure of proteins, depending on the severity of the treatment. Both heat treatment temperature and particle size, as well as their interaction, led to significant changes in $\beta$-sheet number (Table 1). Heat treatment causes a transition of the secondary structure from a loose to an ordered configuration (increased $\beta$-sheet), which promotes molecular aggregation and crosslinking [23]. For L and M particle sizes the increase in temperature determined the rise in $\beta$-sheet structures, while for S fraction the opposite trend was observed (Fig. 4a). L fraction was the richest in $\beta$-sheet structures, followed by M and S particle sizes. Mathematical models for the variation of $\beta$-sheet number with temperature for each particle size are displayed below (eq. 19-21).

L particle:
$\beta - sheet(\%) = 93.78 - 2.31A + 0.02A^2$ (19)
M particle:
$\beta - sheet(\%) = 60.03 - 1.61A + 0.02A^2$ (20)
S particle:
$\beta - sheet(\%) = 46.01 - 1.13A + 0.02A^2$ (21)

The proportion of $\alpha$-helix was affected significantly ($p < 0.05$) by both factors, while their interaction was not significant (Table 1). The increase in temperature led to slight decrease in $\alpha$-helix structures (Fig. 4b). Apparent conformational changes occur at elevated temperatures, accompanied by transitions of secondary structure mainly from $\alpha$-helix to the $\beta$-sheet structures [24]. The highest proportion of $\alpha$-helix conformations was observed in L fraction, followed by S and M. The largest fraction contains the most intact or coarse pieces of the pomace matrix (cell wall remnants, seeds). These larger pieces are more likely to contain undamaged, ordered protein structures. The prediction models for $\alpha$-helix depending on the temperature for each particle size are showed in eq. 22-24.

L particle:
$\alpha - helix\ (\%) = 32.22 - 0.41A + 0.01A^2$ (22)
M particle:
$\alpha - helix\ (\%) = 25.47 - 0.36A + 0.01A^2$ (23)
S particle:
$\alpha - helix\ (\%) = 35.27 - 0.35A + 0.01A^2$ (24)

The proportion of $\beta$-turn conformations was influenced significantly ($p < 0.05$) only by particle size and the interaction between factors, while temperature exhibited a non-significant effect (Table 1). S particle size presented the greatest proportion of $\beta$-turn structures, followed by M and L particle sizes. The mathematical models used to describe the variation of $\beta$-turn structures with temperature for each particle size are displayed below (eq. 25-27).

L particle:
$\beta - turn(\%) = -28.17 + 2.92A - 0.03A^2$(25)
M particle:
$\beta - turn(\%) = -49.5 + 3.03A - 0.03A^2$ (26)
S particle:
$\beta - turn(\%) = -91.00 + 3.49A - 0.03A^2$(27)

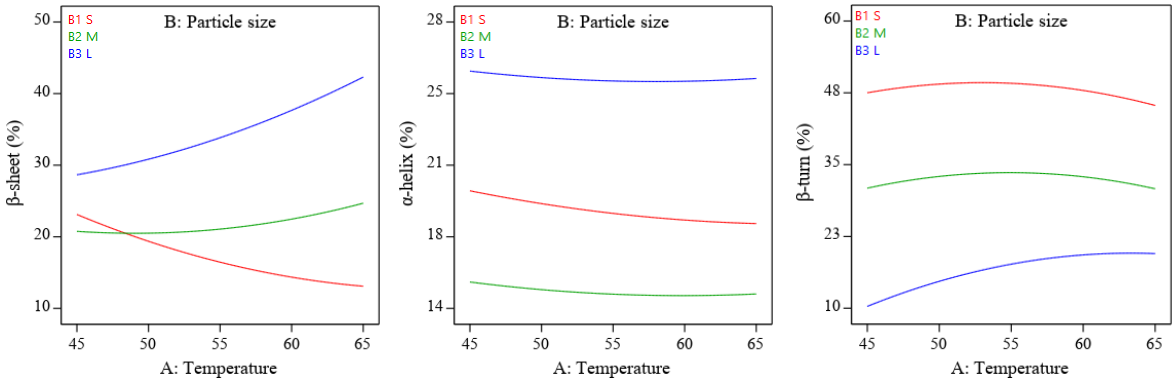


**Fig. 4. Interaction plot of thermal treatment temperature and particle size effects on SBP protein structure**

## 3.2. Correlations

The relationships between SBP characteristics are presented in Fig. 5.

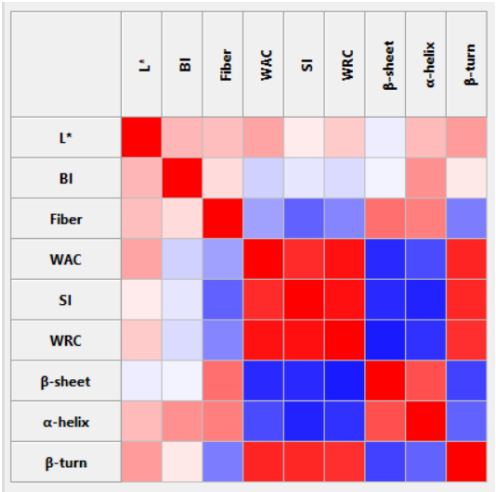


**Fig. 5. Correlations between SBP properties: +1 (red) to -1 (blue) – intensity of the color is proportional with the correlation strength**

Fiber content was moderately negatively correlated with SI ($p < 0.05$). Functional properties (WAC, SI, and WRC) were negatively correlated ($p < 0.05$) with *β*-sheet and *α*-helix protein structures and positively with *β*-turn.

## 3.3. Optimization of the factors

In order to establish the optimal thermal treatment conditions of SBP for each particle size, some constraints were applied (Table 2). Thus, while the two factors were kept in range, the BI, SI, WRC, and *β*-turn were set to be minimal. L* and *α*-helix were set in range, and WAC along with *β*-sheet structures were maximized. All the factors and the variables received the same importance level (Table 2).

**Table 2.**

**Constraints applied for optimization**

| Variable | Goal | Minimum | Maximum | Importance |
|---|---|---|---|---|
| **A: Temperature** | is in range | 45 | 65 | 3 |
| **B: Particle size** | is in range | S (< 200 μm) | L (> 300 μm) | 3 |
| **L*** | is in range | 50.56 | 55.74 | 3 |
| **BI** | minimize | 38.32 | 46.22 | 3 |
| **Fiber (%)** | is in range | 25.73 | 72.64 | 3 |
| **WAC (g/g)** | maximize | 217.87 | 336.18 | 3 |
| **SI (%)** | minimize | 2.99 | 12.31 | 3 |
| **WRC (%)** | minimize | 3.21 | 8.74 | 3 |
| ***β*-sheet (%)** | maximize | 13.06 | 42.30 | 3 |
| ***α*-helix (%)** | is in range | 14.03 | 26.35 | 3 |
| ***β*-turn (%)** | minimize | 10.21 | 54.13 | 3 |

The characteristics of the optimal samples are presented in Table 3. For L fraction, a temperature of 64.82 °C is recommended, while for M fraction, it is 49.48 °C, and for S particle size the optimal temperature is 45.19 °C. The highest BI was observed in OS, while OL presented the highest L*. OL is the richest in fiber content, *β*-sheet and *α*-helix structures, while the WAC, SI, WRC, and *β*-turn values were the smallest compared to the other fractions. OS and OM samples have close values for functional properties, but OS has a higher proportion of *β*-sheet, *α*-helix, and *β*-turn compared to OM.

**Table 3.**

**Characteristics of the optimal samples**

| **Sample** | **OL** | **OM** | **OS** |
|---|---|---|---|
| **Temperature** | 64.82 | 49.48 | 45.19 |
| **Particle size** | L (< 200 μm) | M (200 μm < M <300 μm) | S (> 300 μm) |
| **L*** | 53.91 ± 0.55$^{a}$ | 51.60 ± 0.55$^{b}$ | 53.35 ± 0.55$^{a}$ |
| **BI** | 40.80 ± 0.88$^{b}$ | 39.10 ± 0.88$^{b}$ | 45.07 ± 0.88$^{a}$ |
| **Fiber (%)** | 72.64 ± 2.49$^{a}$ | 25.73 ± 2.49$^{c}$ | 33.66 ± 2.49$^{b}$ |
| **WAC (%)** | 238.61 ± 6.06$^{b}$ | 285.07 ± 6.06$^{a}$ | 275.72 ± 6.06$^{a}$ |
| **SI (%)** | 3.33 ± 0.29$^{b}$ | 10.64 ± 0.29$^{a}$ | 10.63 ± 0.29$^{a}$ |
| **WRC (g/g)** | 3.45 ± 0.36$^{b}$ | 7.18 ± 0.36$^{a}$ | 6.51 ± 0.36$^{a}$ |
| ***β*-sheet (%)** | 42.13 ± 1.75$^{a}$ | 20.50 ± 1.75$^{b}$ | 22.96 ± 1.75$^{b}$ |
| ***α*-helix (%)** | 25.23 ± 0.73$^{a}$ | 14.95 ± 0.73$^{c}$ | 19.72 ± 0.73$^{b}$ |
| ***β*-turn (%)** | 19.52 ± 2.48$^{c}$ | 32.8 ± 2.48$^{b}$ | 47.59 ± 2.48$^{a}$ |

$^{a-c}$ – small letters in the same row indicate significant differences ($p < 0.05$) between samples.

## 4. Conclusion

Thermal treatment conditions and particle size determined significant changes in physical and functional properties of sloe berry pomace. Increasing thermal treatment temperature enhanced lightness (L*), total fiber content, water absorption and retention capacities, and promoted *β*-sheet conformations in proteins depending on the particle size, indicating improved structural stability. However, certain parameters such as solubility index and *β*-turn protein conformations remained unaffected by temperature, suggesting selective thermal sensitivity of SBP components.

Optimization through Response Surface Methodology identified specific ideal drying temperatures for each particle size fraction, 64.82 °C for large (L), 49.48 °C for medium (M), and 45.19 °C for small (S) particles, with the S fraction exhibiting the most desirable color, functional attributes, and protein stability. Overall, the findings confirm that controlled thermal processing combined with appropriate particle size selection can effectively tailor SBP's functional and structural properties. These optimized conditions provide a practical basis for transforming SBP into a high-value ingredient rich in dietary fiber and with superior water-holding capacity, suitable for various applications, thereby supporting sustainable waste valorization in the fruit processing industry.

## 5. Acknowledgments

Mădălina Ungureanu-Iuga and Mariana Spinei were funded by the Romania National Council for Higher Education Funding, CNFIS, project number CNFIS-FDI-2025-F-0603.

## 6. References

[1]. BABALAU-FUSS V., BOGDANA GREBLA O., CADAR O., HOAGHIA M.-A., KOVACS M.-H., MOLDOVAN A., TOFANA M., Determination of Chemical Composition and Fatty Acids of

Blackthorn Fruits (*Prunus Spinosa*) Grown Near Cluj-Napoca, NW Romania, *Agriculture*, 1: 105–106, (2018)
[2]. MUNEKATA P. E. S., YILMAZ B., PATEIRO M., KUMAR M., DOMÍNGUEZ R., SHARIATI M. A., HANO C., LORENZO J. M., Valorization of By-products from *Prunus* Genus Fruit Processing: Opportunities and Applications, *Critical Reviews in Food Science and Nutrition*, 63: 7795–7810, (2023)
[3]. IONESCU A. D., FERDEȘ M., VOICU G., IPATE G., CONSTANTIN G. A., ȘTEFAN E. M., BEGEA M., Effect of Grinding and Successive Sieving on the Distribution of Active Biological Compounds in the Obtained Fractions of Blackthorn Berries, *Applied Sciences*, 14: 1–17, (2024)
[4]. GUNES R., In Vitro Gastrointestinal Digestion of Anthocyanins from Marshmallows Enriched with Blackthorn Fruit Powders Obtained by Convective Hot Air- and Freeze-Drying Treatments, *Food Research International*, 205: 1–12, (2025)
[5]. MAGIERA A., CZERWIŃSKA M. E., OWCZAREK A., MARCHELAK A., GRANICA S., OLSZEWSKA M. A., Polyphenols and Maillard Reaction Products in Dried Prunus Spinosa Fruits: Quality Aspects and Contribution to Anti-Inflammatory and Antioxidant Activity in Human Immune Cells Ex Vivo, *Molecules*, 27: 1–20, (2022)
[6]. DELI M., PETIT J., NGUIMBOU R. M., BEAUDELAIRE DJANTOU E., NJINTANG YANOU N., SCHER J., Effect of Sieved Fractionation on the Physical, Flow and Hydration Properties of *Boscia Senegalensis* Lam., *Dichostachys Glomerata* Forssk. and *Hibiscus Sabdariffa* L. Powders, *Food Science and Biotechnology*, 28: 1375–1389, (2019)
[7]. AL-HILPHY A. R., ALI H. I., AL-IEESSA S. A., GAVAHIAN M., MOUSAVI-KHANEGHAH A., Assessing Compositional and Quality Parameters of Unconcentrated and Refractive Window Concentrated Milk Based on Color Components, *Dairy*, 3: 400–412, (2022)
[8]. OLADIRAN D. A., EMMAMBUX N. M., Nutritional and Functional Properties of Extruded Cassava-Soy Composite with Grape Pomace, *Starch/Staerke*, 70: 1–11, (2018)
[9]. ZHU F., DU B., XU B., Superfine Grinding Improves Functional Properties and Antioxidant Capacities of Bran Dietary Fibre from Qingke (Hull-less Barley) Grown in Qinghai-Tibet Plateau, China, *Journal of Cereal Science*, 65: 43–47, (2015)
[10]. GAO X., TONG J., GUO L., YU L., LI S., YANG B., WANG L., LIU Y., LI F., GUO J., et al., Influence of Gluten and Starch Granules Interactions on Dough Mixing Properties in Wheat (*Triticum Aestivum* L.), *Food Hydrocolloids*, 106: 105885, (2020)
[11]. IUGA M., MIRONEASA S., A Review of the Hydrothermal Treatments Impact on Starch-Based Systems Properties, *Critical Reviews in Food Science and Nutrition*, 60: 3890–3915, (2020)
[12]. MARTI A., BOCK J. E., AMBROGINA M., ISMAIL B., SEETHARAMAN K., Structural Characterization of Proteins in Wheat Flour Doughs Enriched with Intermediate Wheatgrass (*Thinopyrum Intermedium*) Flour, *Food Chemistry*, 194: 994–1002, (2016)
[13]. LI Z., GAN W., HE X., LU H., ZHANG Y., Effect of Particle Size, Transparency and Light Intensity on the Color of Powder, *International Conference on Green Chemistry and Renewable Energy*, 545: 012027, (2020)
[14]. CALABUIG-JIMÉNEZ L., HINESTROZA-CÓRDOBA L. I., BARRERA C., SEGUÍ L., NOELIA BETORET, Effects of Processing and Storage Conditions on Functional Properties of Powdered Blueberry Pomace, *Sustainability*, 14: 1839, (2022)
[15]. SALARI S., FERREIRA J., LIMA A., SOUSA I., Effects of Particle Size on Physicochemical and Nutritional Properties and Antioxidant Activity of Apple and Carrot Pomaces, *Foods*, 13: 1–17, (2024)
[16]. DONG J., YANG M., SHEN R., ZHAI Y., YU X., WANG Z., Effects of Thermal Processing on the Structural and Functional Properties of Soluble Dietary Fiber from Whole Grain Oats, *Food Science and Technology International*, 25: 282–294, (2018)
[17]. CHEN Y., ZHANG B., SUN Y., ZHANG J., SUN H., WEI Z., Physicochemical Properties and Adsorption of Cholesterol by Okra (*Abelmoschus Esculentus*) Powder, *Food & Function*, 6: 1–10, (2015)
[18]. BAMAL P., DHULL S. B., Development of Functional Muffins from Wheat Flour-Carrot Pomace Powder Using Fenugreek Gum as Fat Replacer, *Current Research in Nutrition and Food Science Journal*, 12: 306–319, (2024)
[19]. NASEEM Z., BHAT N. A., MIR S. A., Valorisation of Apple Pomace for the Development of High-Fibre and Polyphenol-Rich Wheat Flour Cookies, *Scientific Reports*, 14: 25912, (2024)
[20]. WODJO D., ADMASSU S., Effects of Pre-Drying Treatment and Particle Sizes on Physicochemical and Structural Properties of Pumpkin Flour, *Heliyon*, 9: e21609, (2023)
[21]. GAO W., CHEN F., ZHANG L., MENG Q., Effects of Superfine Grinding on Asparagus Pomace. Part I: Changes on Physicochemical and Functional Properties, *Journal of Food Science*, 85: 1–7, (2020)

[22]. RICHARDS J., LAMMERT A., MADDEN J., KANG I., AMIN S., Physical Treatments Modified the Functionality of Carrot Pomace, *Foods*, 13: 2084, (2024)
[23]. NIU Q., LIU E., HUO C., ZHANG F., HE R., YANG J., ZHAO Z., Effects of Transglutaminase and Heat Treatment on the Structure and Gelation Properties of Camel Casein Protein, *Foods*, 15: 1644, (2025)
[24]. HU Z., XU Y., GONG Y., KUANG T., Effects of Heat Treatment on the Protein Secondary Structure and Pigment Microenvironment in Photosystem 1 Complex, *Photosynthetica*, 43: 529–534, (2005)